



1 **Low sensitivity of gross primary production to elevated CO<sub>2</sub> in a mature Eucalypt woodland**

2 **Authors:** Jinyan Yang<sup>1</sup>, Belinda E. Medlyn<sup>1</sup>, Martin G. De Kauwe<sup>2,3</sup>, Remko A. Duursma<sup>1</sup>, Mingkai Jiang<sup>1</sup>,  
3 Dushan Kumarathunge<sup>1</sup>, Kristine Y. Crous<sup>1</sup>, Teresa E. Gimeno<sup>4,5</sup>, Agnieszka Wujeska-Klause<sup>1</sup>, David S.  
4 Ellsworth<sup>1</sup>

5

6 **Affiliation:** <sup>1</sup> Hawkesbury Institute for the Environment, Western Sydney University, Penrith, NSW, Australia

7 <sup>2</sup> ARC Centre of Excellence for Climate Extremes, Sydney, NSW 2052, Australia

8 <sup>3</sup> Climate Change Research Centre, University of New South Wales, Sydney, NSW 2052, Australia

9 <sup>4</sup> Basque Centre for Climate Change, Scientific Campus of the University of the Basque Country, Leioa, Spain

10 <sup>5</sup> IKERBASQUE, Basque Foundation for Science, 48008, Bilbao, Spain

11 Correspondence to: Jinyan Yang ([jinyan.yang@westernsydney.edu.au](mailto:jinyan.yang@westernsydney.edu.au))

12

13

14

15 **For submission to: Biogeosciences Discussions**

16 No of words in abstract: 269

17 No of words in main text: 6705

18 No of Figures: 8

19 No of Tables: 1

20

21



22 **Abstract**

23 The response of mature forest ecosystems to rising atmospheric carbon dioxide concentration ( $C_a$ ) is a major  
24 uncertainty in projecting the future trajectory of the Earth's climate. Although leaf-level net photosynthesis is  
25 typically stimulated by exposure to elevated  $C_a$  ( $eC_a$ ), it is unclear how this stimulation translates into carbon  
26 cycle responses at whole-ecosystem scale. Here we estimate a key component of the carbon cycle, the gross  
27 primary productivity (GPP), of a mature native Eucalypt forest exposed to Free Air  $CO_2$  Enrichment (the  
28 EucFACE experiment). In this experiment, light-saturated leaf photosynthesis increased by 19% in response to a  
29 38% increase in  $C_a$ . We used the process-based forest canopy model, MAESPA, to upscale these leaf-level  
30 measurements of photosynthesis with canopy structure to estimate Gross Primary Production (GPP) and its  
31 response to  $eC_a$ . We assessed the direct impact of  $eC_a$ , as well as the indirect effect of photosynthetic  
32 acclimation to  $eC_a$  and variability among treatment plots via different model scenarios.

33 At the canopy scale, MAESPA estimated a GPP of  $1574 \text{ g C m}^{-2} \text{ yr}^{-1}$  under ambient conditions across four years  
34 and a direct increase in GPP of +11% in response to  $eC_a$ . The smaller canopy-scale response simulated by the  
35 model, as compared to the leaf-level response, could be attributed to the prevalence of RuBP-regeneration  
36 limitation of leaf photosynthesis within the canopy. Photosynthetic acclimation reduced this estimated response  
37 to 10%. Considering variability in leaf area index across plots, we estimated a mean GPP response to  $eC_a$  of 6%  
38 with a 95% CI of (-2%, 14%). These findings highlight that the GPP response of mature forests to  $eC_a$  is likely  
39 to be considerably lower than the response of light-saturated leaf photosynthesis. Our results provide an  
40 important context for interpreting  $eC_a$  responses of other components of the ecosystem carbon cycle.



## 41 1. Introduction

42 Forests represent the largest long-term terrestrial carbon storage (Bonan, 2008; Pan et al., 2011). Atmospheric  
43 carbon dioxide concentration ( $C_a$ ) has increased significantly since the beginning of the industrial era (Joos and  
44 Spahni, 2008), but the increase would have been considerably larger without forest carbon sequestration, which  
45 is estimated to have offset 25-33% of recent anthropogenic  $CO_2$  emissions (Le Quéré et al. 2017).  $C_a$  is projected  
46 to continue to increase by 1-5  $\mu\text{mol mol}^{-1}$  per year into the future (IPCC, 2014), but the rate of this rise depends  
47 on the magnitude of the forest feedback on  $C_a$ . At the leaf scale, the direct physiological effects of rising  $C_a$  are  
48 well understood: elevated  $C_a$  ( $eC_a$ ) stimulates plant photosynthesis (Kimball et al. 1993; Ellsworth et al. 2012)  
49 and reduces stomatal conductance (Morison, 1985, Saxe et al. 1998), which together increase leaf water-use  
50 efficiency (De Kauwe et al. 2014). These physiological responses at leaf scale could potentially increase  
51 ecosystem carbon uptake and hence the amount of carbon stored in the ecosystem, which at the global scale  
52 significantly mitigates the rise in  $C_a$ . However, projecting the response of the terrestrial carbon sink to future  
53 increases in  $C_a$  is a major uncertainty in models (Friedlingstein et al. 2014), highlighting an urgent need to make  
54 greater use of data from manipulative experiments at leaf scale to inform terrestrial biosphere models (Medlyn  
55 et al., 2015).

56 Our understanding of ecosystem responses to  $eC_a$  relies on both experiments and observations. However, results  
57 from different types of studies show some important areas of disagreement. At the global scale, satellite data  
58 provide evidence of a strong greening trend over the last 20 years, indicating an increase in leaf area and/or  
59 above-ground biomass, which has been attributed to the gradual increase in  $CO_2$  (Donohue et al., 2009;  
60 Donohue et al., 2013; Yang et al., 2016; Zhu et al., 2016). A positive response of carbon uptake/greenness is  
61 also found in manipulative  $eC_a$  open-top chamber experiments with young trees (Eamus and Jarvis, 1989; Curtis  
62 and Wang 1998; Saxe et al. 1998; Medlyn et al., 1999) and ecosystem-scale FACE experiments in young,  
63 aggrading forest stands (Ainsworth and Long, 2005; Norby et al., 2005; , Ellsworth et al. 2012; Walker et al.  
64 2019). In contrast, individual-tree experiments with mature trees (>30 years old) have found relatively small  
65 responses of tree growth to  $eC_a$  despite an apparent increase in leaf photosynthesis (Dawes et al., 2011;  
66 Sigurdsson et al., 2013; Klein et al., 2016). Also, tree-ring studies indicate an apparent lack of stimulation of  
67 vegetation growth in mature forests over the last century (Peñuelas et al. 2011; Silva and Anand, 2013; van der  
68 Sleen et al. 2014). These studies raise important questions about how mature ecosystems will respond to  $eC_a$ .

69 The Eucalyptus FACE experiment (EucFACE; Australia) is the first replicated, ecosystem-scale experiment  
70 where a mature native forest has been experimentally subjected to  $eC_a$  and provides a valuable case study to  
71 assess the response of a mature forest response to  $eC_a$  under field conditions (Ellsworth et al. 2017). Results  
72 from the first five years (2013-2018) of leaf gas exchange measurements showed a consistent stimulation of  
73 leaf-level light-saturated net photosynthesis ( $A$ ) of 19% (Ellsworth et al., 2017; Wujeska-Klaue et al., 2019).  
74 Nevertheless, the increase in  $A$  did not lead to a detectable change in above-ground growth (Ellsworth et al.,  
75 2017). These experimental results are consistent with empirical evidence arising from tree-ring studies  
76 (Peñuelas et al. 2011; Silva and Anand, 2013; van der Sleen et al. 2014) and also with experimental evidence  
77 from individual mature trees (Körner et al., 2005; Dawes et al., 2011; Klein et al., 2016).



78 As a first step towards reconciling the  $eC_a$  responses of leaf photosynthesis and above-ground growth in this  
79 experiment, here we quantify how the whole canopy carbon uptake, or gross primary productivity (GPP) was  
80 increased under  $eC_a$ . The response of GPP is important because it provides an upper bound on the potential  
81 response of other components of ecosystem carbon balance, such as above-ground growth. It needs to be  
82 quantified explicitly because the response of GPP to  $eC_a$  may be quite different to that of leaf net  
83 photosynthesis. The leaf-level response of photosynthesis to  $eC_a$  is usually measured on sunlit leaves under  
84 saturating light (Ainsworth and Rogers, 2007). As a result, these leaf-level  $eC_a$  responses largely reflect the  
85 responses of the photosynthesis rate when limited by maximum Rubisco activity ( $V_{cmax}$ ). However, depending  
86 on the canopy architecture and ambient light condition, the canopy could have many shaded leaves, which  
87 would mean that the emergent rate of photosynthesis could actually be limited by RuBP regeneration ( $J$ ). RuBP-  
88 regeneration limited photosynthesis has a smaller response to  $eC_a$  than Rubisco-limited photosynthesis  
89 (Ainsworth and Rogers, 2007), resulting in a smaller response of GPP than leaf photosynthesis under saturating  
90 light.

91 The transition from RuBP-regeneration to Rubisco-limited photosynthesis of the canopy is determined by the  
92 ratio of the maximum capacities for RuBP-regeneration and Rubisco activity,  $J_{max}$  and  $V_{cmax}$  (Friend, 2001;  
93 Zaehle et al. 2014; Rogers et al., 2017). Wullschleger (1993) reported a  $J_{max}:V_{cmax}$  ratio of 2, which has been  
94 widely adopted in models (e.g., Wang et al., 1998; Luo et al., 2001; Rogers et al., 2017). However, recent  
95 studies have suggested a lower  $J_{max}:V_{cmax}$  ratio for many forest ecosystems (Kattge and Knorr, 2007; Ellsworth  
96 et al., 2012; Kumarathunge et al., 2018). A lower  $J_{max}:V_{cmax}$  ratio results in more frequent RuBP-regeneration  
97 limitation of photosynthesis, which reduces the response of GPP to  $eC_a$ .

98 It is difficult to directly measure the  $eC_a$  effect on GPP. In some previous  $eC_a$  experiments, GPP has been  
99 estimated by scaling up from leaf-level measurements using a canopy model. Wang et al (1998) and Luo et al  
100 (2001) both used the tree array model, MAESPA, which can simulate the radiative transfer within and between  
101 tree crowns and can be parameterised to describe the spatial locations and sizes of trees in  $eC_a$  experiments. In  
102 these previous applications of MAESPA, the direct response of GPP to  $eC_a$  was consistently half of that  
103 observed at the leaf level because of a large contribution of RuBP-regeneration limited photosynthesis to GPP  
104 (Wang et al., 1998; Luo et al., 2001). However, the direct effect of  $eC_a$  on photosynthesis was modified by two  
105 major indirect effects. When LAI increased under  $eC_a$ , the additional leaf area amplified the GPP response by up  
106 to 60%. The other factor is the downregulation of photosynthesis under  $eC_a$ , or photosynthetic acclimation  
107 (Long et al., 2004; Ainsworth and Rogers, 2007; Rogers, et al., 2017). Under long-term exposure to  $eC_a$ , some  
108 plants have been observed to reduce nitrogen allocation to Rubisco, which results in a decrease of  
109 photosynthetic capacity (Gunderson and Wullschleger, 1993). The average decrease of  $V_{cmax}$  among plants in  
110 FACE experiments was found to be 13% for all species and 6% for trees (Ainsworth and Long, 2005). Both  
111 Wang et al. (1998) and Luo et al. (2001) tested the impact of photosynthetic acclimation and showed a moderate  
112 reduction of canopy GPP (5-6%) due to photosynthetic acclimation (10-20%) at the studied experiments.

113 Following Wang et al. (1998) and Luo et al. (2001), we used MAESPA (Duursma and Medlyn, 2012) to  
114 estimate canopy GPP at EucFACE in ambient and elevated  $C_a$  treatments. The model has previously been  
115 evaluated with leaf- and whole-tree- scale measurements from EucFACE (Yang et al., in review). Here, we first  
116 parameterised the model with physiological, structural and meteorological data measured during the experiment.



117 Then, we quantified the response of canopy GPP to  $eC_a$  and partitioned this response into the direct stimulation  
118 of GPP and the indirect effects of photosynthetic acclimation and variation of LAI. The overall goal of this  
119 study was to estimate the magnitude of the response of forest canopy GPP to  $eC_a$  in order to provide a baseline  
120 against which to compare changes in other components of the ecosystem carbon balance.

## 121 2. Methods

### 122 2.1 Site

123 The EucFACE experiment (technical details in Gimeno et al., 2016) is located in western Sydney, Australia  
124 (33.617S, 150.741E). It consists of six circular plots, each of which has a diameter of 25 m, enclosing 15-25  
125 mature forest trees (referred to as ‘rings’ hereafter). The rings are divided into two groups: control (with ambient  
126  $C_a$ ; 390-400  $\mu\text{mol mol}^{-1}$  during the study period) and experimental ( $eC_a$ ; +150  $\mu\text{mol mol}^{-1}$ ). The tree canopy is  
127 dominated by *Eucalyptus tereticornis* Sm. which are ~20 m in height and have a basal area of ~24  $\text{m}^2 \text{ha}^{-1}$ . The  
128 site receives a mean annual precipitation of 800  $\text{mm yr}^{-1}$ , a mean annual photosynthetically active radiation  
129 (PAR) of 2600  $\text{MJ m}^{-2} \text{yr}^{-1}$ , and a mean annual temperature of 17 °C.

### 130 2.2 Model

131 The MAESPA model is a process-based tree-array model (Wang and Jarvis, 1990) that calculates canopy carbon  
132 and water exchange ([https://bitbucket.org/remkoduursma/maespa/src/Yang\\_et\\_al\\_2019/](https://bitbucket.org/remkoduursma/maespa/src/Yang_et_al_2019/)). At each 30-minute  
133 timestep, the model simulates the radiative transfer, photosynthesis, and transpiration of individual trees  
134 mechanistically. Soil moisture balance can be calculated dynamically, but here we chose to improve accuracy by  
135 using soil moisture as an input to the model (Duursma and Medlyn, 2012).

136 The model represents the tree canopy as an array of tree crowns. The location and dimensions of each crown are  
137 specified based on-site measurements (see 2.3.2 Canopy structure, below). Calculations of carbon and water  
138 fluxes are made for each tree crown, which is divided into six layers. Here it was assumed that crowns are  
139 represented by an ellipsoidal shape and that leaf area is uniformly distributed across layers within the tree  
140 crown. The leaf angles were assumed to follow a spherical distribution to ensure consistency with the method  
141 used to estimate leaf area index (LAI) in Duursma et al. (2016). Within each layer, the model evaluates the  
142 radiation transfer and leaf gas exchange at 12 grid points such that each crown is represented by a total of 72  
143 grid points. The radiation intercepted at each grid point is calculated for direct and diffuse components by  
144 considering shading from the upper crown and surrounding trees and solar angle (zenith and azimuth), and light  
145 source (diffuse or direct). Penetration by direct radiation to each grid point is used to estimate the sunlit and  
146 shaded leaf area at each grid point. The radiation intercepted by the fraction of sunlit and shade foliage is then  
147 used to calculate the leaf gas exchange.

148 The gas exchange sub-model combines the leaf photosynthesis model of Farquhar et al. (1980) with the stomatal  
149 optimisation model, following Medlyn et al. (2011). Stomatal conductance is modelled as:

$$150 \quad g_s = 1.6 \cdot \left(1 + \frac{g_1}{\sqrt{D}}\right) \cdot \frac{A_{\text{net}}}{C_a} \quad (1)$$

151 where  $g_s$  is the stomatal conductance to water vapour ( $\text{mol m}^{-2} \text{s}^{-1}$ );  $g_1$  is a parameter that represents the  $g_s$   
152 sensitivity to photosynthesis ( $\text{kPa}^{0.5}$ ; see definition in Medlyn et al., (2011));  $A_{\text{net}}$  is the net  $\text{CO}_2$  assimilation rate



153 ( $\mu\text{mol m}^{-2} \text{s}^{-1}$ );  $C_a$  is the atmospheric  $\text{CO}_2$  concentration ( $\mu\text{mol mol}^{-1}$ ). The factor 1.6 converts the conductance of  
154  $\text{CO}_2$  to that of  $\text{H}_2\text{O}$ .

155 The impact of soil moisture on  $g_s$  is represented through an empirical function that links soil water availability  
156 to  $g_1$  following (Drake et al., 2017):

$$157 \quad g_1 = g_{1,max} \left( \frac{\theta - \theta_{min}}{\theta_{max} - \theta_{min}} \right)^q \quad (2)$$

158 where the  $g_{1,max}$  is the maximum  $g_1$  value;  $\theta$  is volumetric soil water content (%);  $\theta_{max}$  and  $\theta_{min}$  are the upper and  
159 lower limit within which  $\theta$  has impact on  $g_1$ ;  $q$  describes the non-linearity of the curve. The equations to  
160 calculate  $A_{net}$  are in Supplementary (Text S1, Eqns. S1 – S6).

161 Following Yang et al. (2019), MAESPA considers a non-stomatal limitation to biochemical parameters  $J_{max}$  and  
162  $V_{cmax}$  at high  $D$ :

$$163 \quad V_{max} = V_{max,t} (1 - c_D \cdot D) \quad (3)$$

164 where  $V_{max,t}$  is the  $J_{max}$  or  $V_{cmax}$  at given leaf temperature, and  $c_D$  is a fitted parameter (Table 1). This relationship  
165 is empirical and fitted to data collected in EucFACE. Incorporating this relationship was shown to improve the  
166 predicted photosynthesis by the leaf gas exchange model (Yang et al., 2019).

167 Combining Eqns. 1-3 and S1 – S6 yields the  $g_s$  and  $A_{net}$  of each grid point, which is then multiplied by leaf area  
168 at each grid point and summed to give whole-tree photosynthesis. Photosynthesis of individual trees is then  
169 summed to give whole-canopy photosynthesis.

## 170 2.3 Model Parameterisation

### 171 2.3.1 Meteorological forcing

172 The model is driven by *in situ* PAR, wind speed, air temperature, vapour pressure deficit ( $D$ ), and soil moisture  
173 measurements from 2013 to 2016 (Figures 1 and 2). The PAR, air temperature, and relative humidity were  
174 measured every five minutes in each ring and then were gap-filled by linear interpolation and aggregated to 30  
175 minute-mean time slices across all six rings (Figure 1). Each ring has a set of PAR (LI-190, Li-cor, Lincoln, NE,  
176 U.S.), wind speed (WinCAP Ultrasonic WMT700 Vaisala, Vantaa, Finland), humidity, and temperature sensors  
177 (HUMICAP © HMP 155 Vaisala, Vantaa, Finland) at the centre of the ring above the canopy at 23.5 m.  $D$  was  
178 calculated from temperature and humidity measurements.

179 Two levels of  $C_a$  were used in the model according to the measured  $C_a$  (LI-840, Li-cor, Lincoln, NE, U.S.). The  
180 ambient  $C_a$  was gap-filled (in total <10 days during four years gaps due to power outage) and aggregated to 30  
181 minute-mean time slices from the five-minute measurements across the three ambient rings (rings 2, 3, and 6).  
182 The  $eC_a$  was processed in the same way but using data from the experimental rings (rings 1, 4, and 5).

183 The volumetric soil water content ( $\theta$ ) was used as an estimate of plant water availability and was taken every 20  
184 days using neutron measurements at 25 cm intervals (503DR Hydroprobe, Instroteck, NC, U.S.) and averaged to  
185 the top 150 cm (Figure 2). There were two probes in each ring and the average of these probes was used to  
186 represent the ring average for each measurement date.  $\theta$  was updated on the days of measurements and thus not  
187 gap-filled.



### 188 2.3.2 Canopy structure

189 Trees in MAESPA were represented by their actual location, height, and crown size to mimic the realistic  
190 effects of shading. Tree location, crown height, crown base and stem diameter were measured in January 2013  
191 at the start of the experiment. For each ring, a time-series of LAI was obtained based on measurements of  
192 above- and below- canopy PAR (Duursma et al. 2016). This LAI represents plant area index, which includes the  
193 woody component as well as leaves and does not account for clumping. In order to retrieve the actual LAI, we  
194 assumed a constant branch and stem cover ( $0.8 \text{ m}^2 \text{ m}^{-2}$ ) based on the lowest LAI during November 2013 when  
195 the canopy shed almost all leaves. The LAI used in this study was thus the plant area index estimates from  
196 Duursma et al. (2016), less  $0.8 \text{ m}^2 \text{ m}^{-2}$  (Figure 2a). Since LAI is the only parameter beside soil moisture that  
197 differed by ring, canopy structure (i.e., the LAI and its distribution) was the major driver of inter-ring  
198 variability.

199 The total leaf area ( $\text{m}^2$ ) of each ring was calculated as the product of LAI and ground area of each plot ( $491 \text{ m}^2$ ).  
200 This total leaf area (LA) was then assigned to each tree based on an allometric relationship between the total leaf  
201 area ( $\text{m}^2$ ) and diameter at breast height (DBH; m). The allometric relationship was derived from data in the  
202 BAAD database (Falster et al., 2015) for *Eucalyptus* trees grown in natural conditions with  $\text{DBH} < 1 \text{ m}$  to match  
203 the characteristics of EucFACE. In total, this database yielded a total of 66 observations with which to estimate  
204 the relationship between LA and DBH:

$$205 \quad L_{\text{allom}} = a \cdot \text{DBH}^b \quad (4)$$

206 where  $L_{\text{allom}}$  is the theoretical leaf area based on allometric relationship to DBH. The values obtained via fitting  
207 for  $a$  and  $b$  were 492.6 and 1.8 respectively, with a root mean square error of  $14.4 \text{ (m}^2\text{)}$ . This relationship was  
208 used to assign the total LA of each ring to each tree in the following steps: (i) the  $L_{\text{allom}}$  for each tree was  
209 calculated based on DBH; (ii) the  $L_{\text{allom}}$  was summed to obtain a total LA for each ring; and (iii) the fractional  
210 contribution of each tree to the ring total LA was calculated. The total LA based on LAI was then assigned to  
211 each tree based on this fraction.

212 The crown radius was calculated with a linear function with DBH based on measurements made in August  
213 2016. The data consisted of DBH and crown radius (one on North-South axis and one on East-west axis) of four  
214 trees in each ring. The crown radius measurements were averaged by tree and used to fit a linear model with  
215 DBH. The estimated slope and intercept of the relationship are  $0.095 \text{ (m cm}^{-1}\text{)}$  and  $0.765 \text{ (m)}$ , respectively.

216 MAESPA also considered the shading from surrounding trees outside the rings. However, no measurements of  
217 locations or diameters were available for the trees surrounding the rings. Therefore, a total of 80 surrounding  
218 trees were arbitrarily assumed to form two uniform and circular layers around each ring. They were assigned the  
219 mean height, mean crown radius, and mean leaf area estimated from all trees in EucFACE. Except for shading,  
220 the surrounding trees have no impact on the trees within the rings. Ring 1 is shown in Figure S1 as an example  
221 of the representation of canopy structure in MAESPA.

### 222 2.3.3 Physiology

223 The physiological parameters were estimated from field gas exchange measurements as described below. The  
224 data were collected with portable photosynthesis systems (Li-6400, Li-Cor, Inc., USA). The only parameter



225 found to differ between ambient and elevated  $C_a$  rings was  $V_{\text{cmax},25}$  ( $V_{\text{cmax}}$  at 25 °C; Ellsworth et al., in prep.).  
226 Hence, all other parameters (e.g., the temperature responses of photosynthesis and respiration) were estimated  
227 by combining all data across  $\text{CO}_2$  treatments. Fitted parameter values are given in Table 1.

228 A set of temperature-controlled photosynthesis- $\text{CO}_2$  response ( $A-C_i$ ) curves was measured at different leaf  
229 temperatures (20-40 °C) under saturating light in February 2016. The dataset was used to quantify the  
230 temperature dependences of  $J_{\text{max}}$  and  $V_{\text{cmax}}$  by fitting a peaked Arrhenius function (Eqn. S5) to the  
231 measurements. We assumed that these temperature response functions applied throughout the period of the  
232 study.

233 Light- and temperature-controlled  $A-C_i$  curves were also measured in the morning for ten field campaigns  
234 during 2013 to 2016. All  $A-C_i$  curves were started at the growth  $C_a$  of 395  $\mu\text{mol mol}^{-1}$  or 545  $\mu\text{mol mol}^{-1}$   
235 (depending on  $eC_a$  treatment) with a saturating light of 1800  $\mu\text{mol m}^{-2} \text{s}^{-1}$  and a flow rate of 500  $\mu\text{mol s}^{-1}$  with  
236 temperature controlled to a constant based on the seasonal temperature. These data were used to estimate  $J_{\text{max}}$   
237 and  $V_{\text{cmax}}$  at 25 °C using the *fitaci* function in the *plantecophys* R package (Duursma, 2015), using the measured  
238 temperature responses of  $J_{\text{max}}$  and  $V_{\text{cmax}}$  described in the previous paragraph to correct to 25 °C.

239 Repeated gas exchange measurements were made on the same leaves in the morning and afternoon under  
240 prevailing field conditions and saturating light (photon flux density = 1800  $\mu\text{mol m}^{-2} \text{s}^{-1}$ ) on four occasions in  
241 2013 (“diurnal”; Gimeno et al., 2016). To expand the diurnal dataset, we obtained the points from  $A-C_i$  curves at  
242 field  $C_a$  and combined the two data sets. These data were used to estimate the  $g_1$  parameter in the stomatal  
243 conductance model (Eqn. 1) using the *fitBB* function in the *plantecophys* R package (Duursma, 2015). One  $g_1$   
244 value was fitted to the data from each treatment and date. The  $g_1$  values were then regressed against  $\theta$  measured  
245 in each treatment group to estimate the impact of soil moisture availability on leaf gas exchange, following Eqn.  
246 2. The  $g_1$  values were related to the nearest measurements of  $\theta$  (within two weeks without rain). Eqn. 2 was  
247 fitted to this data set using the non-linear least squares method (Figure 3).

248 The dark respiration rate of foliage,  $R_{\text{dark}}$ , was measured at least three hours after sunset at a range of leaf  
249 temperatures (14-60 °C) in February 2016 also with LiCor 6400. The temperature dependence of  $R_{\text{dark}}$  was fitted  
250 using non-linear least squared method to all of the measured data using Eqn. S6. Light responses of  
251 photosynthesis were measured on two trees from each ring in October 2014 (Crous et al., unpublished). This  
252 data set was used to constrain the light response parameters ( $\alpha_j$  and  $\theta_j$ ) in Eqn. S4. Details of fitting the light  
253 response curves are provided in supplementary (Text S1).

#### 254 **2.4 Model simulations and analysis**

255 MAESPA was used to simulate radiation interception and gas exchange of all six rings between 1 January 2013  
256 and 31 December 2016 on a half-hourly basis. The model simulated half-hourly gross primary production (GPP)  
257 of each tree, which was then summed for all trees in each ring to get the total annual GPP for each ring and year.

258 Four different sets of simulations were used to estimate carbon uptake under ambient and  $eC_a$  and to identify the  
259 key limiting factors on canopy GPP response to  $eC_a$ . Firstly, we carried out a simulation of leaf scale (“leaf  
260 scenario”) photosynthesis with measured meteorological data but fixed physiological data ( $g_1 = 3.3 \text{ kPa}^{0.5}$ ,  
261  $V_{\text{cmax},25} = 91 \mu\text{mol m}^{-2} \text{s}^{-1}$ , and  $J_{\text{max},25} = 159 \mu\text{mol m}^{-2} \text{s}^{-1}$ ). This simulation aimed to quantify the  $\text{CO}_2$  response of  
262 Rubisco-limited and RuBP-limited photosynthesis at the leaf scale. This calculation was made using the



263 *photosyn* function in *plantecophys* R package (Duursma, 2015). This function implements the leaf gas exchange  
 264 routine used in MAESPA.

265 Secondly, MAESPA was run for all six rings with ambient  $C_a$  and with  $V_{cmax,25}$  from ambient measurements  
 266 (“ambient scenario”). The results of this simulation were used to calculate the GPP of each ring under ambient  
 267 conditions. The ambient GPP values were also used to evaluate the inherent variability among the rings.

268 Thirdly, all six rings were simulated with  $eC_a$  and  $V_{cmax,25}$  based on measurements from ambient rings (“elevated  
 269 scenario”). The results of this simulation were compared to those from the ambient scenario to illustrate the  
 270 instantaneous response of canopy GPP to  $eC_a$  in each ring and year. This simulation also quantifies the variation  
 271 of the GPP response to  $eC_a$  across rings and years.

272 Lastly, we simulated the response of the three rings exposed to  $eC_a$  (rings 1, 4, and 5) using the  $V_{cmax,25}$  and  $eC_a$   
 273 measured from these elevated rings (“field scenario”). Results from the field scenario were used for two  
 274 analyses: (i) to compare GPP from the field scenario to that of the three rings from the elevated scenario (i.e.,  
 275  $eC_a$  and ambient  $V_{cmax,25}$ ), which allows us to quantify the impact of photosynthetic acclimation (i.e., due to a  
 276 reduction in  $V_{cmax}$ ); (ii) to calculate the difference in GPP between the three ambient rings in ambient scenario  
 277 and elevated rings in the field scenario to estimate the response of GPP to  $eC_a$  in the field.

278 *Table 1. Summary table of parameter definitions, units, and sources used in this study.*

Parameters	Definitions	Units	Values	Eqn.
$\alpha_j$	Quantum yield of electron transport rate	$\mu\text{mol } \mu\text{mol}^{-1}$	0.30	S7
$a$	Fitted slope of LA and DBH	$\text{m}^2 \text{m}^{-1}$	492.6	4
$a_{\text{abs}}$	Absorptance of PAR	fraction	0.825	S4
$b$	Fitted index of LA and DBH	-	1.8	4
$c_D$	Slope of $V_{cmax}$ to $D$	$\text{kPa}^{-1}$	0.14	3
$\Delta S$	Entropy factor	$\text{J mol}^{-1} \text{K}^{-1}$	639.60 ( $V_{cmax}$ ); 638.06 ( $J_{max}$ )	S5
$E_a$	Activation energy	$\text{J mol}^{-1}$	66386 ( $V_{cmax}$ ); 32292 ( $J_{max}$ )	S5
$g_{1,max}$	Maximum $g_1$ value	$\text{kPa}^{0.5}$	5.0	2
$H_d$	Deactivation energy	$\text{J mol}^{-1}$	200000	S5
$\theta_1$	Convexity of electron transport rate to $Q_{\text{APAR}}$	-	0.48	S8
$\theta_{max}$	Upper limit which $\theta$ has impact on $g_1$	-	0.240	2
$\theta_{min}$	Lower limit which $\theta$ has impact on $g_1$	-	0.106	2
$J_{max,25}$	Value of $J_{max}$ at 25°C	$\mu\text{mol m}^{-2} \text{s}^{-1}$	159	3
$k_T$	Sensitivity of $R_{dark}$ to temperature	$^{\circ}\text{C}^{-1}$	0.078	S6
$q$	The non-linearity of the $g_1$ dependence of $\theta$	-	0.425	2
$R_{day,25}$	Light respiration rate	$\mu\text{mol m}^{-2} \text{s}^{-1}$	0.9	S6
$R_{dark,25}$	Dark respiration rate	$\mu\text{mol m}^{-2} \text{s}^{-1}$	1.3	S6
$R_{gas}$	Gas constant	$\text{J mol}^{-1} \text{K}^{-1}$	8.314	S5
$V_{cmax,25}$	Value of $V_{cmax}$ at 25°C	$\mu\text{mol m}^{-2} \text{s}^{-1}$	91 (ambient); 83 (elevated)	3

279



### 280 3. Results

281 Figure 4 summarises the results from measurements and the different simulations conducted in this study. It  
282 demonstrates that the impact of  $eC_a$  diminishes as calculations are scaled from the instantaneous leaf-level  
283 response ( $A_{inst}$ ) to the long-term canopy response ( $GPP_{field}$ ) and the various feedback effects are accounted for.  
284 Each row of Figure 4 is explained in detail in the following paragraphs.

#### 285 3.1 Instantaneous $C_a$ response of photosynthesis at leaf and canopy scale

286 The mean instantaneous  $C_a$  response of leaf-level photosynthesis ( $A_{inst}$ ) was +33% (Figure 4a). This response  
287 ratio was calculated from ~600 light- and temperature-controlled  $A-C_i$  curves measured in the ambient rings.  
288 From the curves, we extracted the photosynthesis at 400 and 550  $C_a$  ( $\mu\text{mol mol}^{-1}$ ) and calculated the  
289 instantaneous  $C_a$  effect as their ratio. This approach allows an estimation of the direct  $\text{CO}_2$  response independent  
290 of the impact of photosynthetic acclimation.

291 By contrast, the modelled direct GPP response to  $eC_a$  was considerably less, just +11%, as shown in Figure 4d  
292 (“GPP<sub>inst</sub>”). This canopy response rate was calculated by comparing the modelled GPP of all six rings under  
293 ambient and elevated  $C_a$  (“ambient” vs. “elevated” scenario). As a result, this direct canopy GPP response also  
294 excludes the impact of photosynthetic acclimation.

295 Our results show that the major reason for the difference between the direct leaf and canopy photosynthesis  
296 responses to  $eC_a$  is the relative contributions from Rubisco- and RuBP-regeneration-limited photosynthesis (cf.  
297 Figure 4 b and c). Figure 5 shows that the response of photosynthesis to  $eC_a$  is considerably higher when  
298 Rubisco activity limits photosynthesis ( $A_c$ ) than when RuBP-regeneration limits photosynthesis ( $A_j$ ). When  
299 averaged over the range of leaf temperatures experienced during the four years of experiment, the  $A_c$  response to  
300  $eC_a$  on average (+26%; Figure 4b) is larger than that of  $A_j$  (+10%; Figure 4c). Leaf gas exchange measurements  
301 were taken in saturating light ( $1800 \mu\text{mol m}^{-2} \text{s}^{-1}$ ) and thus, are mostly Rubisco limited. The observed response  
302 rate of  $A_{inst}$  is thus close to that of  $A_c$ .

303 At the canopy scale, a large fraction of the modelled canopy photosynthesis is limited by RuBP-regeneration. In  
304 Figure 6, we show the distribution of  $A_c$  and  $A_j$  during the four years of simulation as calculated by MAESPA.  
305 On average, 70% of the canopy photosynthesis is limited by RuBP-regeneration under ambient conditions  
306 (“ambient scenario”). The high fraction of  $A_j$  is partly a consequence of the relatively low ratio of  $J_{max,25}$  to  
307  $V_{max,25}$  (J:V ratio) which was estimated to be 1.7 (Table 1). In Figure 7, we estimated the PAR level at which  
308 Rubisco activity becomes limiting to leaf photosynthesis. The transition point from Rubisco- to RuBP-  
309 regeneration-limited photosynthesis was calculated from the leaf gas exchange sub-model by assuming a  
310 constant  $C_a$  ( $390 \mu\text{mol mol}^{-1}$ ),  $D$  (1.5 kPa),  $g_l$  ( $3.3 \text{ kPa}^{0.5}$ ), and  $V_{max,25}$  ( $90 \mu\text{mol m}^{-2} \text{s}^{-1}$ ) but varying leaf  
311 temperature. As shown, under these conditions, when temperature = 25 °C and J:V ratio = 1.7, Rubisco activity  
312 limits photosynthesis only when incident PAR >  $1800 \mu\text{mol m}^{-2} \text{s}^{-1}$ . Using a higher J:V ratio such as the  
313 commonly-used value of 2 would decrease the saturating PAR value at which photosynthesis becomes Rubisco  
314 limited. We ran additional simulations assuming a J:V ratio of 2 and found that, with this ratio, MAESPA  
315 estimated 48% of photosynthesis to be RuBP-regeneration limited under ambient conditions and a direct GPP  
316 response of 15% (data not shown).



317 The shape of the light response curve also determines the transition point from RuBP- to Rubisco-limited  
318 photosynthesis. We explored this effect by investigating the effect of varying the convexity,  $\theta_j$ . At EucFACE,  
319 this parameter is estimated to be 0.48 based on data collected on site, indicating a shallow curvature and a high  
320 light saturation points, in contrast to the commonly assumed 0.85, representing a steeper curvature and a lower  
321 light saturation point. Using a value of 0.85 for  $\theta_j$  resulted in a much lower PAR required for photosynthesis to  
322 become Rubisco limited (dashed curves in Figure 7). With a  $\theta_j$  of 0.85 and a J:V ratio of 1.7, MAESPA  
323 estimated 40% of photosynthesis to be RuBP-regeneration limited under ambient conditions and a direct GPP  
324 response of 16% (data not shown). With a  $\theta_j$  of 0.85 and a J:V ratio of 2, MAESPA estimated just 34% of  
325 photosynthesis to be RuBP-regeneration limited under ambient conditions and a direct GPP response of 18%  
326 (Figure S2). The simulated CO<sub>2</sub> response of canopy carbon uptake thus depends heavily on the parameterisation  
327 of light response and J:V ratio.

328

### 329 3.2 Acclimation of photosynthesis

330 The above calculations are made considering only the instantaneous response of photosynthesis to  $eC_a$ .  
331 However, photosynthetic acclimation was observed at leaf scale (Ellsworth et al., in prep), and will also reduce  
332 the response of GPP to  $eC_a$  at the canopy scale. At the leaf-level, photosynthesis measured in the elevated rings  
333 after five years of treatment ( $A_{long}$ ) was 19% higher than that measured in ambient rings (Figure 4e; Ellsworth et  
334 al. 2017).  $A_{long}$  thus accounts for the photosynthetic acclimation in the elevated rings after four years of exposure  
335 to  $eC_a$ .  $A_{long}$  is considerably smaller than  $A_{inst}$  (19% vs. 33%; Figure 4 a and e), indicating a large effect of  
336 photosynthetic acclimation on the  $eC_a$  response of light-saturated photosynthesis.

337 Accounting for the impact of photosynthetic acclimation in MAESPA, by using the  $V_{cmax}$  from elevated rings  
338 (“field” vs. “ambient” scenarios) reduced the response of GPP to  $C_a$  from 11% to 10% ( $GPP_{long}$ ; Figure 4f). As  
339 such, the photosynthetic acclimation had a relatively modest impact on the modelled annual GPP in the model.  
340 The small impact of photosynthetic acclimation on canopy photosynthesis relative to the effect on leaf  
341 photosynthesis can be explained by the fact that the leaf photosynthesis data are measured under saturating light  
342 and thus are typically Rubisco-limited, so a reduction in  $V_{cmax}$  had a large effect. In contrast, at the canopy scale,  
343 much of the photosynthesis was limited by RuBP-regeneration and was largely unaffected by a reduction in  
344  $V_{cmax}$ .

### 345 3.3 Influence of LAI

346 The realised GPP response to  $eC_a$  also depends on the canopy structure, specifically the LAI. In this experiment,  
347 there was no significant change in LAI with  $eC_a$  ( $-4\% \pm 5\%$ ; Figure 4g; see also Duursma et al. 2016). The  
348 effect of  $eC_a$  on LAI was calculated as the average effect between elevated and ambient annual mean LAI.  
349 However, there was inherent variability in LAI across the rings (Figure 2a), which does not fundamentally  
350 change the effect of  $eC_a$  but requires a detailed analysis of the potential effects of natural variability on the  
351 response to  $eC_a$ .

352



353 The small pre-treatment difference in LAI across rings gives rise to a range of estimates for the GPP response to  
354  $eC_a$  in the field ( $6\% \pm 8\%$ ; Figure 4h). This result is explored further in Figure 8, which combines the results  
355 from “ambient”, “elevated”, and “field” scenarios. The average GPP across all six rings under ambient  $C_a$  was  
356  $1574 \text{ g C m}^{-2} \text{ yr}^{-1}$  over the four-year simulation (“ambient scenario”; Figure 8). However, there was significant  
357 variability in ambient GPP across rings, related in part to the inherent variability in LAI across rings. We  
358 characterised the pre-existing differences in LAI by the initial LAI ( $LAI_i$ ), measured on 26 October 2012. These  
359 initial values are low, because they are measured immediately before the seasonal leaf flush, but characterise the  
360 difference in LAI across rings over the full experimental period. Rings 1 and 4 (both experimental rings) have  
361 the lowest  $LAI_i$  ( $<0.3 \text{ m}^2 \text{ m}^{-2}$ ) and thus the lowest average GPP under ambient conditions ( $1206 \text{ g C m}^{-2} \text{ yr}^{-1}$ ).  
362 Ring 5 (the other experimental ring) has the second highest  $LAI_i$  ( $\sim 0.4 \text{ m}^2 \text{ m}^{-2}$ ) and also the highest GPP under  
363 ambient conditions ( $2359 \text{ g C m}^{-2} \text{ yr}^{-1}$ ). The variability among rings in ambient GPP ( $SD = 15\%$ ) is thus larger  
364 than the modelled direct effect of  $C_a$  on GPP, which is similar in all rings ( $+11\%$ ).

365 Owing to the variability among rings represented by  $LAI_i$ , the estimated mean GPP response to  $eC_a$  across the  
366 experimental rings has a sizeable confidence interval ( $\pm 8\%$ , Figure 4h). The actual  $eC_a$  response was estimated  
367 as an average effect between the ambient and elevated GPP values considering the impacts of photosynthetic  
368 acclimation and inter-ring variability. The average GPP of experimental rings under field conditions ( $eC_a$ ) was  
369 estimated to be  $1698 \text{ g C m}^{-2} \text{ yr}^{-1}$  while the average GPP of control rings under field conditions (ambient  $C_a$ )  
370 was  $1599 \text{ g C m}^{-2} \text{ yr}^{-1}$ , an increase of  $6\%$  as shown in the Figure 4h. The variation of annual average GPP of the  
371 control and experimental groups (blue and red squares in Figure 8) are thus represented by the CI in Figure 4h.

372

#### 373 4. Discussion

374 We have showed how a large response of leaf-level photosynthesis to  $eC_a$  diminishes when integrated to the  
375 canopy-scale, according to the synthesis of four years of leaf measurements at EucFACE with the stand-scale  
376 model, MAESPA. We estimated that the canopy GPP of a mature *Eucalyptus* woodland under ambient  $C_a$   
377 conditions varied from  $1084\text{--}2129 \text{ g C m}^{-2} \text{ yr}^{-1}$  by ring and year with a mean of  $1574 \text{ g C m}^{-2} \text{ yr}^{-1}$ . The model,  
378 constrained by site measurements, predicted that once scaled to the canopy, the response of GPP to  $eC_a$  only  
379 increased by  $6\%$  ( $95\% \text{ CI of } \pm 8\%$ ) compared to the  $19\%$  ( $95\% \text{ CI of } \pm 5\%$ ) observed in leaf-scale measurements.  
380 We were able to quantify the response of GPP to  $eC_a$  and attribute the reduction in the response to various  
381 factors including: (i) Rubisco versus RuBP-regeneration limitations to photosynthesis; (ii) photosynthetic  
382 acclimation; (iii) inter-ring variability in LAI. Together these findings provide valuable insights into the relative  
383 importance of each factor and help close a key knowledge gap in our understanding of how mature forests  
384 respond to  $eC_a$ .

##### 385 4.1 Performance of MAESPA under ambient conditions

386 The ambient GPP of EucFACE estimated by MAESPA was comparable to that measured with eddy covariance  
387 in similar evergreen Eucalypt forests in Southeast Australia. In a nearby eddy covariance site ( $<1 \text{ km}$ ),  
388 Renchon et al. (2018) estimated the ecosystem GPP from eddy covariance to be  $1561 \text{ g C m}^{-2} \text{ yr}^{-1}$  during 2013  
389 to 2016 which is within the range estimated for the ambient rings in this study, though this latter site and the  
390 EucFACE are not the same in terms of canopy structure and LAI. Furthermore, our version of MAESPA was



391 evaluated against leaf photosynthesis and whole-tree sap flow measurements in EucFACE ( $R^2$  of 0.77 and 0.8,  
392 respectively; Yang et al., in review). These comparisons indicate MAESPA is a useful tool to explore the  
393 canopy carbon uptake and the predicted GPP could provide a baseline to future studies.

#### 394 **4.2 RuBP-regeneration limited photosynthesis**

395 Our results show that the canopy GPP at EucFACE was predominantly limited by RuBP regeneration. The  
396 reason for the frequent RuBP-regeneration limitation is that the measured J:V ratio was relatively small in  
397 EucFACE (1.7), and stomata tend to close at midday when light levels are higher and Rubisco-limitation is  
398 expected (Gimeno et al., 2016). A lower J:V ratio increases the PAR threshold required for the photosynthesis  
399 model to switch between the RuBP-regeneration limitation and the Rubisco limitation (from  $<1000$  to  $<1800$   
400  $\mu\text{mol m}^{-2} \text{s}^{-1}$ ; Figure 7). Previous studies have highlighted the need to consider J:V ratio for a correct prediction  
401 of  $\text{CO}_2$  response (Long et al, 2004; Zaehle et al., 2014; Rogers et al., 2017). However, as shown by Zaehle et al.  
402 (2014), Medlyn et al. (2015), and Rogers et al. (2017), current models differ in their predictions of the transition  
403 from RuBP-regeneration- to Rubisco-limited photosynthesis, suggesting the uncertainty of predicted  $\text{CO}_2$   
404 response of GPP could be reduced by using a realistic J:V ratio.

405 Previous modelling studies applying MAESPA to  $eC_a$  experiments both assumed higher J:V ratio (2) and  
406 estimated higher GPP response to  $eC_a$  presumably due to less frequent RuBP-regeneration limitation (Wang et  
407 al., 1998; Luo et al., 2001). A J:V ratio of 2 was suggested by Wullschleger (1993) and has been used in many  
408 modelling studies (e.g., the seven terrestrial biosphere models assessed by Rogers et al. (2017) all assumed a J:V  
409 ratio of 1.9-2). Global terrestrial biosphere models such as JULES and others frequently estimate  $J_{\text{max}}$  on the  
410 basis of this ratio (e.g., Clark et al. 2011). However, the relatively low J:V ratio observed at EucFACE is not  
411 unique. In the Duke Forest FACE site in the US, Ellsworth et al. (2012) reported a J:V ratio of  $\sim 1.7$  which is the  
412 same as that estimated for EucFACE. Kattge and Knorr (2007) analysed  $V_{\text{cmax}}$  and  $J_{\text{max}}$  values from 36 species  
413 across the world and found a low J:V ratio ( $<1.8$ ) in herbaceous, coniferous, and broadleaved species. Most  
414 recently, Kumarathunge et al. (2018) studied the variation in J:V ratio in datasets obtained from around the  
415 globe and found a consistent relationship with growing season temperature. The ratio varied from 2.5 in tundra  
416 environments to  $< 1.5$  in tropical environments. The value of 1.7 observed at EucFACE falls within this  
417 prediction for the prevailing growth temperature at this site. The inclusion of his relationship between this  
418 relationship of J:V ratio and temperature will thus be important for capturing the GPP response to  $eC_a$  globally.

419 We also found that the curvature of the light response of photosynthesis affected the predicted GPP response to  
420  $eC_a$  (Figure 7). The parameter value we fitted to data measured *in situ* ( $\theta_j = 0.48$ ) is lower than the value  
421 commonly assumed in the models (typically around 0.85, e.g. Medlyn et al., 2002; Harverd et al., 2018).  
422 Nonetheless, our relatively low  $\theta_j$  value ( $<0.7$ ) is not unique, as it is also supported by a number of studies on  
423 different species around the world (Ögren, 1993; Valladares et al., 1997; Lewis et al., 2000; Hjelm and Ögren,  
424 2004). The inclusion of higher  $\theta_j$  value would predict a much higher direct GPP response to  $eC_a$  (e.g., 16%  
425 versus 11% in this study), because higher  $\theta_j$  results in a large proportion of GPP being Rubisco-limited. This  
426 finding calls for careful examination of the light-response of photosynthesis, which has a large effect on the  
427 predicted  $eC_a$  response



#### 428 **4.2 Photosynthetic acclimation**

429 Some degree of photosynthetic acclimation (i.e., a long-term reduction of  $V_{\text{cmax}}$  under  $eC_a$ ) has been widely  
430 reported in FACE studies and has been attributed to a reduction of leaf nitrogen concentration (Saxe et al., 1998;  
431 Ainsworth and Long, 2005). The response of GPP to  $eC_a$  would be linearly related to  $V_{\text{cmax}}$  if photosynthesis  
432 were mostly limited by Rubisco activity. Photosynthetic acclimation was responsible for the reduced response of  
433 leaf-scale light-saturated photosynthesis from 33% ( $A_{\text{inst}}$ ) to 19% ( $A_{\text{long}}$ ). However, this reduction in  $V_{\text{cmax}}$   
434 translated into only a ~2% reduction in GPP modelled by MAESPA. Wang et al. (1998) also showed that  
435 photosynthetic acclimation (-21% in  $V_{\text{cmax}}$ ) reduced modelled canopy GPP by only 6% due to RuBP-  
436 regeneration being the primary limitation of canopy photosynthesis. These findings thus suggest that  
437 photosynthetic acclimation may only have a small effect in the GPP response to  $eC_a$  when canopy  
438 photosynthesis is mostly RuBP-regeneration limited. This response is thus consistent with the hypothesis that  
439 the reduction in  $V_{\text{cmax}}$  represents a re-allocation of nitrogen to optimise nitrogen use efficiency under  $eC_a$  (Chen  
440 et al., 1993; Medlyn et al., 1996).

#### 441 **4.3 Constraining the carbon balance response to $eC_a$**

442 At EucFACE, after four years of  $eC_a$  treatment, there was no evidence of increased above-ground tree growth  
443 (Ellsworth et al., 2017). Nor have the trees at EucFACE shown any significant change in LAI (Duursma et al.,  
444 2016). The relatively small response of GPP and the effect of ring-to-ring variation provides important context  
445 for these statistically non-significant responses of tree growth at the stand scale at EucFACE. Firstly, the effect  
446 size calculated for GPP of +11% (+ 169 g C m<sup>-2</sup> yr<sup>-1</sup>) constrains the likely effect size for plant growth and other  
447 components of the ecosystem carbon balance and is a more useful baseline for comparison than the response of  
448 light-saturated leaf photosynthesis (+19% = 299 g C).

449 Secondly, the inherent ring-to-ring variation in this natural forest stand is even higher than the GPP response,  
450 which highlights the importance of considering both the effect size and uncertainty than to focus on statistical  
451 significance. It is important to note that the EucFACE site could be considered relatively homogeneous for a  
452 mature woodland. The site is flat, trees appear similar-aged, and almost all the overstorey belongs to a single  
453 species. In addition, plots were carefully sited to minimise variation in basal area. However, there are small-  
454 scale variations in soil type, depth, and nutrient availability that cause variation in LAI. This scale of variation is  
455 likely to present in other natural forests, and indeed, other studies on mature trees also note that background  
456 variability can contribute to the lack of statistically significant findings (Fatichi and Leuzinger, 2013;  
457 Sigurdsson et al. 2013). We highlight the need to focus on effect size and its uncertainty, rather than the  
458 dichotomous significant/non-significant approach when evaluating experimental results from native forests.

#### 459 **4.4 Implications for terrestrial biosphere models**

460 Seven Terrestrial Biosphere Models (TBMs) were used to predict GPP and LAI responses to  $eC_a$  in advance of  
461 the EucFACE experiment (Medlyn et al. 2016). The predicted  $eC_a$  responses of GPP ranged from +2 to +24%  
462 across the seven models, while the predicted responses of LAI ranged from +1 to +20%. With our results, it is  
463 possible to falsify some of these model simulations. The model with the lowest GPP response (CLM4-P)  
464 assumed very strong down-regulation of photosynthesis owing to phosphorus limitation. However, this down-  
465 regulation was not observed here. The models with the highest GPP responses (GDAY, O-CN, SDGVM) had a



466 J:V ratio of 2 which is higher than that observed at EucFACE, and also had a positive feedback to GPP via  
467 increased LAI (+5-15%), which did not occur (Duursma et al., 2016). The model rendering most similar  
468 prediction for the GPP response to  $eC_a$  to the output of MAESPA incorporating empirical observations was the  
469 CABLE model. This latter model predicted an  $eC_a$  response of GPP of ~12% with a large proportion of RuBP-  
470 regeneration limited photosynthesis, both of which are similar to the findings in this study. Future TBMs may  
471 benefit from incorporating a more realistic representation of the relative contribution of RuBP-regeneration- to  
472 Rubisco- limited photosynthesis to GPP. For instance, adding the temperature dependency of J:V ratio could  
473 help capture the variation of J:V ratio globally (e.g., Kumarathunge et al., 2018).

474 Our study provides a number of process-based insights that can be used to improve model performance both  
475 qualitatively and quantitatively. Our modelling exercise is also a major contribution to the understanding of the  
476 EucFACE experiment by quantifying the amount of extra carbon input into the system by canopy-level  
477 photosynthesis and thus providing a reference for assessing the impacts of  $eC_a$  on growth and soil respiration.  
478 Finally, our study highlights that the  $eC_a$  effect on canopy-scale GPP may be considerably lower than the effect  
479 on photosynthesis of the light-saturated leaves, due to contrasting relative limitations to photosynthesis  
480 operating and different scales. In future work, our GPP estimates will be used as an input to calculate the overall  
481 effect of  $eC_a$  on the carbon balance at the whole EucFACE site.

#### 482 **Acknowledgements**

483 JY was supported by a PhD scholarship from Hawkesbury Institute for the Environment, Western Sydney  
484 University. MGDK was supported by NSW Research Attraction and Acceleration Program (RAAP).

485 EucFACE was built as an initiative of the Australian Government as part of the Nation-building Economic  
486 Stimulus Package and is supported by the Australian Commonwealth in collaboration with Western Sydney  
487 University. It is also part of a TERN Super-site facility.

488 We thank Vinod Kumar, Craig McNamara and Craig Barton, for their excellent technical support. We also  
489 thank Elise Dando for help in measuring crown radius, Steven Wohl for crane driving, Julia Cooke and Burhan  
490 Amiji for installing the neutron probe access tubes.

#### 491 **Author contribution statement**

492 JY, BM, MDK, and RD conceived and designed the analysis. KC, DE, and TG designed sampling of leaf  
493 physiological data, while DE and RD designed sampling of canopy structure data. KC, DE, TG, AWK, RD and  
494 JY collected data. RD and DK provided analysis tools. JY and BM performed the analysis. JY, BM, MDK, and  
495 MJ wrote the paper. All authors edited and approved the manuscript.

496

497

#### 498 **References**

499 Ainsworth, E. A. and Long, S. P.: What have we learned from 15 years of free-air CO<sub>2</sub> enrichment (FACE)? A  
500 meta-analytic review of the responses of photosynthesis, canopy properties and plant production to rising CO<sub>2</sub>,  
501 *New Phytol.*, 165(2), 351–372, doi:10.1111/j.1469-8137.2004.01224.x, 2005.



- 502 Bernacchi, C. J., Singaas, E. L., Pimentel, C., Portis Jr, A. R. and Long, S. P.: Improved temperature response  
503 functions for models of Rubisco-limited photosynthesis, *Plant, Cell Environ.*, 24(2), 253–259,  
504 doi:10.1046/j.1365-3040.2001.00668.x, 2001.
- 505 Bonan, G. B. and Doney, S. C.: Climate, ecosystems, and planetary futures: The challenge to predict life in  
506 Earth system models, *Science* (80-), 359(6375), doi:10.1126/science.aam8328, 2018.
- 507 Chen, J. L., Reynolds, J. F., Harley, P. C. and Tenhunen, J. D.: Coordination theory of leaf nitrogen distribution  
508 in a canopy, *Oecologia*, 93(1), 63–69, doi:10.1007/BF00321192, 1993.
- 509 Clark, D. B., Mercado, L. M., Sitch, S., Jones, C. D., Gedney, N., Best, M. J., Pryor, M., Rooney, G. G., Essery,  
510 R. L. H., Blyth, E., Boucher, O., Harding, R. J., Huntingford, C. and Cox, P. M.: The Joint UK Land  
511 Environment Simulator (JULES), model description – Part 2: Carbon fluxes and vegetation dynamics, *Geosci.  
512 Model Dev.*, 4(3), 701–722, doi:10.5194/gmd-4-701-2011, 2011.
- 513 Curtis, P. S., and X. Wang (1998), A meta-analysis of elevated CO<sub>2</sub> effects on woody plant mass, form, and  
514 physiology, *Oecologia*, 113(3), 299–313, doi:10.1007/s004420050381.
- 515 Dawes, M. A., Hättenschwiler, S., Bebi, P., Hagedorn, F., Handa, I. T., Körner, C. and Rixen, C.: Species-  
516 specific tree growth responses to 9 years of CO<sub>2</sub> enrichment at the alpine treeline, *J. Ecol.*, 99(2), 383–394,  
517 doi:10.1111/j.1365-2745.2010.01764.x, 2011.
- 518 De Kauwe, M. G., Medlyn, B. E., Zaehle, S., Walker, A. P., Dietze, M. C., Wang, Y. P., Luo, Y., Jain, A. K.,  
519 El-Masri, B., Hickler, T., Wårlind, D., Weng, E., Parton, W. J., Thornton, P. E., Wang, S., Prentice, I. C., Asao,  
520 S., Smith, B., Mccarthy, H. R., Iversen, C. M., Hanson, P. J., Warren, J. M., Oren, R. and Norby, R. J.: Where  
521 does the carbon go? A model-data intercomparison of vegetation carbon allocation and turnover processes at  
522 two temperate forest free-air CO<sub>2</sub> enrichment sites, *New Phytol.*, 203(3), 883–899, doi:10.1111/nph.12847,  
523 2014.
- 524 Donohue, R. J., McVicar, T. R. and Roderick, M. L.: Climate-related trends in Australian vegetation cover as  
525 inferred from satellite observations, 1981–2006, *Glob. Chang. Biol.*, 15(4), 1025–1039, doi:10.1111/j.1365-  
526 2486.2008.01746.x, 2009.
- 527 Donohue, R. J., Roderick, M. L., McVicar, T. R. and Farquhar, G. D.: Impact of CO<sub>2</sub> fertilization on maximum  
528 foliage cover across the globe’s warm, arid environments, *Geophys. Res. Lett.*, 40(12), 3031–3035,  
529 doi:10.1002/grl.50563, 2013.
- 530 Drake, J. E., Power, S. A., Duursma, R. A., Medlyn, B. E., Aspinwall, M. J., Choat, B., Creek, D., Eamus, D.,  
531 Maier, C., Pfautsch, S., Smith, R. A., Tjoelker, M. G. and Tissue, D. T.: Stomatal and non-stomatal limitations  
532 of photosynthesis for four tree species under drought: A comparison of model formulations, *Agric. For.  
533 Meteorol.*, 247, 454–466, doi:10.1016/j.agrformet.2017.08.026, 2017.
- 534 Duursma, R. A. and Medlyn, B. E.: MAESPA: a model to study interactions between water limitation,  
535 environmental drivers and vegetation function at tree and stand levels, with an example application to [CO<sub>2</sub>] ×  
536 drought interactions, *Geosci. Model Dev.*, 5(4), 919–940, doi:10.5194/gmd-5-919-2012, 2012.
- 537 Duursma, R. A.: Plantecophys - An R package for analysing and modelling leaf gas exchange data, *PLoS One*,  
538 10(11), 1–13, doi:10.1371/journal.pone.0143346, 2015.
- 539 Duursma, R. A., Gimeno, T. E., Boer, M. M., Crous, K. Y., Tjoelker, M. G. and Ellsworth, D. S.: Canopy leaf  
540 area of a mature evergreen *Eucalyptus* woodland does not respond to elevated atmospheric [CO<sub>2</sub>] but tracks  
541 water availability, *Glob. Chang. Biol.*, 22(4), 1666–1676, doi:10.1111/gcb.13151, 2016.
- 542 Eamus, D. and Jarvis, P. G.: The direct effects of increase in the global atmospheric CO<sub>2</sub> concentration on natural  
543 and commercial temperate trees and forests, *Advances in Ecological Research*, vol. 19, pp. 1–55., 1989.



- 544 Ellsworth, D. S., Thomas, R., Crous, K. Y., Palmroth, S., Ward, E., Maier, C., Delucia, E. and Oren, R.:  
545 Elevated CO<sub>2</sub> affects photosynthetic responses in canopy pine and subcanopy deciduous trees over 10 years: A  
546 synthesis from Duke FACE, *Glob. Chang. Biol.*, 18(1), 223–242, doi:10.1111/j.1365-2486.2011.02505.x, 2012.
- 547 Ellsworth, D. S., Anderson, I. C., Crous, K. Y., Cooke, J., Drake, J. E., Gherlenda, A. N., Gimeno, T. E.,  
548 Macdonald, C. A., Medlyn, B. E., Powell, J. R., Tjoelker, M. G. and Reich, P. B.: Elevated CO<sub>2</sub> does not  
549 increase eucalypt forest productivity on a low-phosphorus soil, *Nat. Clim. Chang.*, 7(4), 279–282,  
550 doi:10.1038/nclimate3235, 2017.
- 551 Farquhar, G. D., Caemmerer, S. and Berry, J. A.: A biochemical model of photosynthetic CO<sub>2</sub> assimilation in  
552 leaves of C3 species, *Planta*, 149(1), 78–90, doi:10.1007/BF00386231, 1980.
- 553 Faticchi, S. and Leuzinger, S.: Reconciling observations with modeling: The fate of water and carbon allocation  
554 in a mature deciduous forest exposed to elevated CO<sub>2</sub>, *Agric. For. Meteorol.*, 174–175, 144–157,  
555 doi:10.1016/j.agrformet.2013.02.005, 2013.
- 556 Friend, A.: Modelling canopy CO<sub>2</sub> fluxes: are ‘big-leaf’ simplifications justified?, *Glob. Ecol. Biogeogr.*, 10(6),  
557 603–619, 2001.
- 558 Gimeno, T. E., Crous, K. Y., Cooke, J., O’Grady, A. P., Ósvaldsson, A., Medlyn, B. E. and Ellsworth, D. S.:  
559 Conserved stomatal behaviour under elevated CO<sub>2</sub> and varying water availability in a mature woodland, *Funct.  
560 Ecol.*, 30(5), 700–709, doi:10.1111/1365-2435.12532, 2016.
- 561 Gimeno, T. E., McVicar, T. R., O’Grady, A. P., Tissue, D. T. and Ellsworth, D. S.: Elevated CO<sub>2</sub> did not affect  
562 the hydrological balance of a mature native *Eucalyptus* woodland, *Glob. Chang. Biol.*, 33(0), 0–2,  
563 doi:10.1111/gcb.14139, 2018.
- 564 Haverd, V., Smith, B., Nieradzki, L., Briggs, P. R., Woodgate, W., Trudinger, C. M., Canadell, J. G. and Cuntz,  
565 M.: A new version of the CABLE land surface model (Subversion revision r4601) incorporating land use and  
566 land cover change, woody vegetation demography, and a novel optimisation-based approach to plant  
567 coordination of photosynthesis, *Geosci. Model Dev.*, 11(7), 2995–3026, doi:10.5194/gmd-11-2995-2018, 2018.
- 568 Hjelm, U. and Ögren, E.: Photosynthetic responses to short-term and long-term light variation in *Pinus*  
569 *sylvestris* and *Salix dasyclados*, *Trees*, 18(6), 622–629, doi:10.1007/s00468-004-0329-8, 2004.
- 570 IPCC, 2014: Climate Change 2014: Synthesis Report. Contribution of Working Groups I, II and III to the Fifth  
571 Assessment Report of the Intergovernmental Panel on Climate Change [Core Writing Team, R.K. Pachauri and  
572 L.A. Meyer (eds.)]. *IPCC*, Geneva, Switzerland, 151 pp.
- 573 Joos, F. and Spahni, R.: Rates of change in natural and anthropogenic radiative forcing over the past 20,000  
574 years, *Proc. Natl. Acad. Sci.*, 105(5), 1425–1430, doi:10.1073/pnas.0707386105, 2008.
- 575 Knauer, J., Zaehle, S., De Kauwe, M. G., Bahar, N. H. A., Evans, J. R., Medlyn, B. E., Reichstein, M. and  
576 Werner, C.: Effects of mesophyll conductance on vegetation responses to elevated CO<sub>2</sub> concentrations in a land  
577 surface model, *Glob. Chang. Biol.*, (September 2018), 1–19, doi:10.1111/gcb.14604, 2019.
- 578 Keenan, T. F., Hollinger, D. Y., Bohrer, G., Dragoni, D., Munger, J. W., Schmid, H. P. and Richardson, A. D.:  
579 Increase in forest water-use efficiency as atmospheric carbon dioxide concentrations rise, *Nature*, 499(7458),  
580 324–327, doi:10.1038/nature12291, 2013.
- 581 Kimball, B. A., Mauney, J. R., Nakayama, F. S. I. and Idso, S. B.: Effects of increasing atmospheric CO<sub>2</sub> on  
582 vegetation, *Vegetatio*, 104/105, 65–75 [online] Available from:  
583 <https://link.springer.com/article/10.1007/BF00048145>, 1993.



- 584 Klein, T., Bader, M. K. F., Leuzinger, S., Mildner, M., Schleppi, P., Siegwolf, R. T. W. and Körner, C.: Growth  
585 and carbon relations of mature *Picea abies* trees under 5 years of free-air CO<sub>2</sub> enrichment, edited by E. Lines, *J.*  
586 *Ecol.*, 104(6), 1720–1733, doi:10.1111/1365-2745.12621, 2016.
- 587 Körner, C., Asshoff, R., Bignucolo, O., Hattenschwiler, S., Keel, S. G., Pelaez-Riedl, S., Pepin, S., Siegwolf, R.  
588 T. W. and Zotz, G.: Carbon flux and growth in mature deciduous forest trees exposed to elevated CO<sub>2</sub>, *Science*  
589 (80), 309(5739), 1360–1362, 2005.
- 590 Kumarathunge, D. P., Medlyn, B. E., Drake, J. E., Tjoelker, M. G., Aspinwall, M. J., Battaglia, M., Cano, F. J.,  
591 Carter, K. R., Cavaleri, M. A., Cernusak, L. A., Chambers, J. Q., Crous, K. Y., De Kauwe, M. G., Dillaway, D.  
592 N., Dreyer, E., Ellsworth, D. S., Ghannoum, O., Han, Q., Hikosaka, K., Jensen, A. M., Kelly, J. W. G., Kruger,  
593 E. L., Mercado, L. M., Onoda, Y., Reich, P. B., Rogers, A., Slot, M., Smith, N. G., Tarvainen, L., Tissue, D. T.,  
594 Togashi, H. F., Tribuzy, E. S., Uddling, J., Vårhammar, A., Wallin, G., Warren, J. M. and Way, D. A.:  
595 Acclimation and adaptation components of the temperature dependence of plant photosynthesis at the global  
596 scale, *New Phytol.*, 222(2), 768–784, doi:10.1111/nph.15668, 2019.
- 597 Le Quéré, C., Andrew, R. M., Friedlingstein, P., Sitch, S., Pongratz, J., Manning, A. C., Korsbakken, J. I.,  
598 Peters, G. P., Canadell, J. G., Jackson, R. B., Boden, T. A., Tans, P. P., Andrews, O. D., Arora, V. K., Bakker,  
599 D. C. E., Barbero, L., Becker, M., Betts, R. A., Bopp, L., Chevallier, F., Chini, L. P., Ciais, P., Cosca, C. E.,  
600 Cross, J., Currie, K., Gasser, T., Harris, I., Hauck, J., Haverd, V., Houghton, R. A., Hunt, C. W., Hurtt, G.,  
601 Ilyina, T., Jain, A. K., Kato, E., Kautz, M., Keeling, R. F., Klein Goldewijk, K., Körtzinger, A., Landschützer,  
602 P., Lefèvre, N., Lenton, A., Lienert, S., Lima, I., Lombardozi, D., Metzl, N., Millero, F., Monteiro, P. M. S.,  
603 Munro, D. R., Nabel, J. E. M. S., Nakaoka, S., Nojiri, Y., Padín, X. A., Peregon, A., Pfeil, B., Pierrot, D.,  
604 Poulter, B., Rehder, G., Reimer, J., Rödenbeck, C., Schwinger, J., Séférian, R., Skjelvan, I., Stocker, B. D.,  
605 Tian, H., Tilbrook, B., van der Laan-Luijkx, I. T., van der Werf, G. R., van Heuven, S., Viovy, N., Vuichard, N.,  
606 Walker, A. P., Watson, A. J., Wiltshire, A. J., Zaehle, S. and Zhu, D.: Global Carbon Budget 2017, *Earth Syst.*  
607 *Sci. Data Discuss.*, (November), 1–79, doi:10.5194/essd-2017-123, 2017.
- 608 Lewis, J. D., McKane, R. B., Tingey, D. T. and Beedlow, P. A.: Vertical gradients in photosynthetic light  
609 response within an old-growth Douglas-fir and western hemlock canopy, *Tree Physiol.*, 20(7), 447–456,  
610 doi:10.1093/treephys/20.7.447, 2000.
- 611 Long, S. P., Ainsworth, E. A., Rogers, A. and Ort, D. R.: Rising atmospheric carbon dioxide: Plants FACE the  
612 Future, *Annu. Rev. Plant Biol.*, 55(1), 591–628, doi:10.1146/annurev.arplant.55.031903.141610, 2004.
- 613 Luo, Y., Medlyn, B., Hui, D., Ellsworth, D., Reynolds, J. and Katul, G.: Gross primary productivity in duke  
614 forest: Modeling synthesis of CO<sub>2</sub> experiment and eddy-flux data, *Ecol. Appl.*, 11(1), 239–252,  
615 doi:10.2307/3061070, 2001.
- 616 Medlyn, B. E.: Interactive effects of atmospheric carbon dioxide and leaf nitrogen concentration on canopy light  
617 use efficiency: A modeling analysis, *Tree Physiol.*, 16(1–2), 201–209, doi:10.1093/treephys/16.1-2.201, 1996.
- 618 Medlyn, B., Badeck, F.-W., De Pury, D., Barton, C., Broadmeadow, M., Ceulemans, R., De Angelis, P.,  
619 Forstreuter, M., Jach, M., Kellomäki, S., Laitat, E., Marek, M., Philippot, S., Rey, A., Strassmeyer, J., Laitinen,  
620 K., Liozon, R., Portier, B., Robertntz, P., Wang, K. and Jarvis, P.: Effects of elevated [CO<sub>2</sub>] on photosynthesis  
621 in European forest species: a meta-analysis of model parameters, *Plant Cell Environ.*, 22, 1475–1495, 1999.
- 622 Medlyn, B. E., De Kauwe, M. G., Zaehle, S., Walker, A. P., Duursma, R. A., Luus, K., Mishurov, M., Pak, B.,  
623 Smith, B., Wang, Y. P., Yang, X., Crous, K. Y., Drake, J. E., Gimeno, T. E., Macdonald, C. A., Norby, R. J.,  
624 Power, S. A., Tjoelker, M. G. and Ellsworth, D. S.: Using models to guide field experiments: *a priori*  
625 predictions for the CO<sub>2</sub> response of a nutrient- and water-limited native *Eucalypt* woodland, *Glob. Chang. Biol.*,  
626 22(8), 2834–2851, doi:10.1111/gcb.13268, 2016.
- 627 Medlyn, B. E., Dreyer, E., Ellsworth, D., Forstreuter, M., Harley, P. C., Kirschbaum, M. U. F., Le Roux, X.,  
628 Montpied, P., Strassmeyer, J., Walcroft, a., Wang, K. and Loustau, D.: Temperature response of parameters of



- 629 a biochemically based model of photosynthesis. II. A review of experimental data, *Plant, Cell Environ.*, 25(9),  
630 1167–1179, doi:10.1046/j.1365-3040.2002.00891.x, 2002.
- 631 Medlyn, B. E., Duursma, R. A., Eamus, D., Ellsworth, D. S., Prentice, I. C., Barton, C. V. M., Crous, K. Y., De  
632 Angelis, P., Freeman, M. and Wingate, L.: Reconciling the optimal and empirical approaches to modelling  
633 stomatal conductance, *Glob. Chang. Biol.*, 17(6), 2134–2144, doi:10.1111/j.1365-2486.2010.02375.x, 2011.
- 634 Medlyn, B. E., Zaehle, S., De Kauwe, M. G., Walker, A. P., Dietze, M. C., Hanson, P. J., Hickler, T., Jain, A.  
635 K., Luo, Y., Parton, W., Prentice, I. C., Thornton, P. E., Wang, S., Wang, Y. P., Weng, E., Iversen, C. M.,  
636 Mccarthy, H. R., Warren, J. M., Oren, R. and Norby, R. J.: Using ecosystem experiments to improve vegetation  
637 models, *Nat. Clim. Chang.*, 5(6), 528–534, doi:10.1038/nclimate2621, 2015.
- 638 Morison, J. I. L.: Sensitivity of stomata and water use efficiency to high CO<sub>2</sub>, *Plant, Cell Environ.*, 8, 467–474,  
639 1985. Niinemets, Ü., Keenan, T. F. and Hallik, L.: A worldwide analysis of within-canopy variations in leaf  
640 structural, chemical and physiological traits across plant functional types, *New Phytol.*, 205(3), 973–993,  
641 doi:10.1111/nph.13096, 2015.
- 642 Norby, R. J., DeLucia, E. H., Gielen, B., Calfapietra, C., Giardina, C. P., King, J. S., Ledford, J., McCarthy, H.  
643 R., Moore, D. J. P., Ceulemans, R., De Angelis, P., Finzi, A. C., Karnosky, D. F., Kubiske, M. E., Lukac, M.,  
644 Pregitzer, K. S., Scarascia-Mugnozza, G. E., Schlesinger, W. H. and Oren, R.: Forest response to elevated CO<sub>2</sub>  
645 is conserved across a broad range of productivity, *Proc. Natl. Acad. Sci.*, 102(50), 18052–18056,  
646 doi:10.1073/pnas.0509478102, 2005.
- 647 Ögren, E.: Convexity of the Photosynthetic Light-Response Curve in Relation to Intensity and Direction of  
648 Light during Growth., *Plant Physiol.*, 101(3), 1013–1019 [online] Available from:  
649 <http://www.ncbi.nlm.nih.gov/pubmed/12231754> <http://www.pubmedcentral.nih.gov/articlerender.fcgi?artid=PMC158720>, 1993.
- 651 Pan, Y., Birdsey, R. A., Fang, J., Houghton, R., Kauppi, P. E., Kurz, W. A., Phillips, O. L., Shvidenko, A.,  
652 Lewis, S. L., Canadell, J. G., Ciais, P., Jackson, R. B., Pacala, S. W., McGuire, A. D., Piao, S., Rautiainen, A.,  
653 Sitch, S. and Hayes, D.: A large and persistent carbon sink in the world's forests, *Science* (80), 333(6045), 988–  
654 993, doi:10.1126/science.1201609, 2011.
- 655 Peñuelas, J., Canadell, J. G. and Ogaya, R.: Increased water-use efficiency during the 20th century did not  
656 translate into enhanced tree growth, *Glob. Ecol. Biogeogr.*, 20(4), 597–608, doi:10.1111/j.1466-  
657 8238.2010.00608.x, 2011.
- 658 Saxe, H., Ellsworth, D. S. and Heath, J.: Tree and forest functioning in an enriched CO<sub>2</sub> atmosphere, *New  
659 Phytol.*, 139(3), 395–436, doi:10.1046/j.1469-8137.1998.00221.x, 1998.
- 660 Sigurdsson, B. D., Medhurst, J. L., Wallin, G., Eggertsson, O. and Linder, S.: Growth of mature boreal Norway  
661 spruce was not affected by elevated [CO<sub>2</sub>] and/or air temperature unless nutrient availability was improved, *Tree  
662 Physiol.*, 33(11), 1192–1205, doi:10.1093/treephys/tpt043, 2013.
- 663 Silva, L. C. R. and Anand, M.: Probing for the influence of atmospheric CO<sub>2</sub> and climate change on forest  
664 ecosystems across biomes, *Glob. Ecol. Biogeogr.*, 22(1), 83–92, doi:10.1111/j.1466-8238.2012.00783.x, 2013.
- 665 Slevin, D., Tett, S. F. B. and Williams, M.: Multi-site evaluation of the JULES land surface model using global  
666 and local data, *Geosci. Model Dev.*, 8(2), 295–316, doi:10.5194/gmd-8-295-2015, 2015.
- 667 Valladares, F., Allen, M. T. and Percy, R. W.: Photosynthetic responses to dynamic light under field conditions  
668 in six tropical rainforest shrubs occurring along a light gradient, *Oecologia*, 111(4), 505–514,  
669 doi:10.1007/s004420050264, 1997.



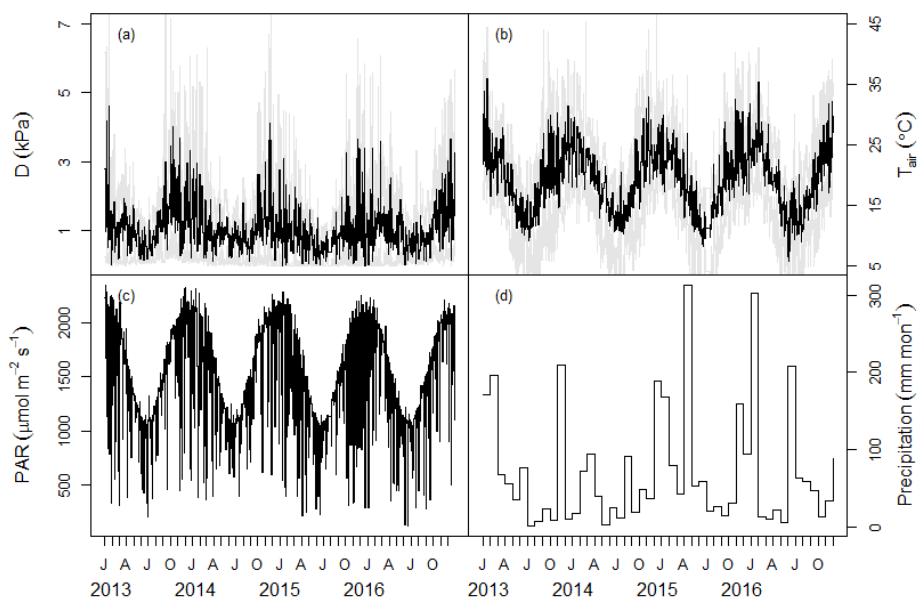
- 670 van der Sleen, P., Groenendijk, P., Vlam, M., Anten, N. P. R., Boom, A., Bongers, F., Pons, T. L., Terburg, G.  
671 and Zuidema, P. A.: No growth stimulation of tropical trees by 150 years of CO<sub>2</sub> fertilization but water-use  
672 efficiency increased, *Nat. Geosci.*, 8(1), 24–28, doi:10.1038/ngeo2313, 2015.
- 673 Walker, A. P., De Kauwe, M. G., Medlyn, B. E., Zaehle, S., Iversen, C. M., Asao, S., Guenet, B., Harper, A.,  
674 Hickler, T., Hungate, B. A., Jain, A. K., Luo, Y., Lu, X., Lu, M., Luus, K., Megonigal, J. P., Oren, R., Ryan, E.,  
675 Shu, S., Talhelm, A., Wang, Y.-P., Warren, J. M., Werner, C., Xia, J., Yang, B., Zak, D. R. and Norby, R. J.:  
676 Decadal biomass increment in early secondary succession woody ecosystems is increased by CO<sub>2</sub> enrichment,  
677 *Nat. Commun.*, 10(1), 454, doi:10.1038/s41467-019-08348-1, 2019.
- 678 Wang, Y. P., Rey, A. and Jarvis, P. G.: Carbon balance of young birch trees grown in ambient and elevated  
679 atmospheric CO<sub>2</sub> concentrations, *Glob. Chang. Biol.*, 4(8), 797–807, doi:10.1046/j.1365-2486.1998.00170.x,  
680 1998.
- 681 Wujeska-Klaue, A., Crous, K. Y., Ghannoum, O. and Ellsworth, D. S.: Lower photorespiration in elevated CO<sub>2</sub>  
682 reduces leaf N concentrations in mature *Eucalyptus* trees in the field, *Glob. Chang. Biol.*, (August 2018), 1–14,  
683 doi:10.1111/gcb.14555, 2019.
- 684 Wullschlegel, S. D.: Biochemical Limitations to Carbon Assimilation in C<sub>3</sub> Plants—A Retrospective Analysis  
685 of the A/C<sub>i</sub> Curves from 109 Species, *J. Exp. Bot.*, 44(5), 907–920, doi:10.1093/jxb/44.5.907, 1993.
- 686 Yang, J., Medlyn, B. E., De Kauwe, M. G. and Duursma, R. A.: Applying the concept of ecohydrological  
687 equilibrium to predict steady state leaf area index, *J. Adv. Model. Earth Syst.*, 10(8), 1740–1758,  
688 doi:10.1029/2017MS001169, 2018.
- 689 Zaehle, S., Medlyn, B. E., De Kauwe, M. G., Walker, A. P., Dietze, M. C., Hickler, T., Luo, Y., Wang, Y. P.,  
690 El-Masri, B., Thornton, P., Jain, A., Wang, S., Warlind, D., Weng, E., Parton, W., Iversen, C. M., Gallet-  
691 Budynek, A., Mccarthy, H., Finzi, A., Hanson, P. J., Prentice, I. C., Oren, R. and Norby, R. J.: Evaluation of 11  
692 terrestrial carbon-nitrogen cycle models against observations from two temperate Free-Air CO<sub>2</sub> Enrichment  
693 studies, *New Phytol.*, 202(3), 803–822, doi:10.1111/nph.12697, 2014.
- 694 Zhu, Z., Piao, S., Myneni, R. B., Huang, M., Zeng, Z., Canadell, J. G., Ciais, P., Sitch, S., Friedlingstein, P.,  
695 Arneeth, A., Liu, R., Mao, J., Pan, Y., Peng, S., Peñuelas, J. and Poulter, B.: Greening of the Earth and its  
696 drivers, *Nat. Clim. Chang.*, 6, early online, doi:10.1038/NCLIMATE3004, 2016.
- 697



698 **Figures and Captions**

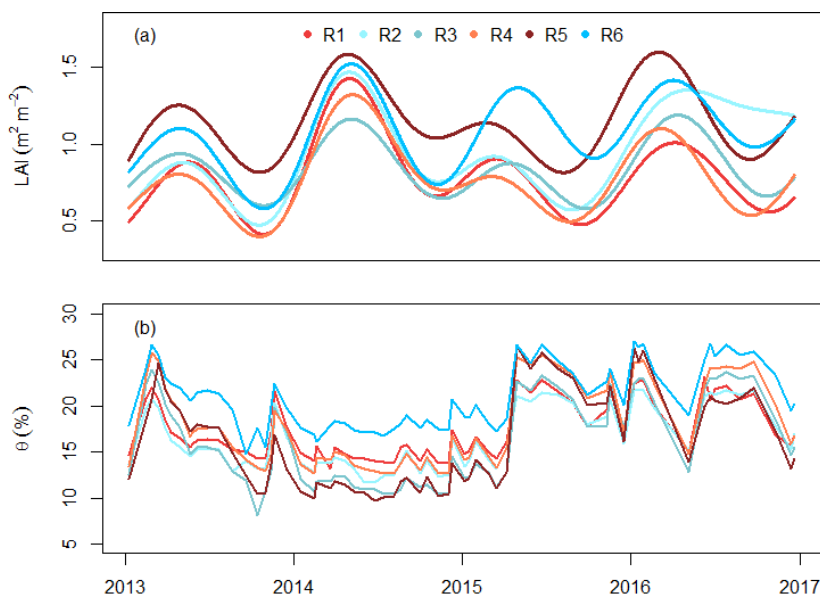
699

700



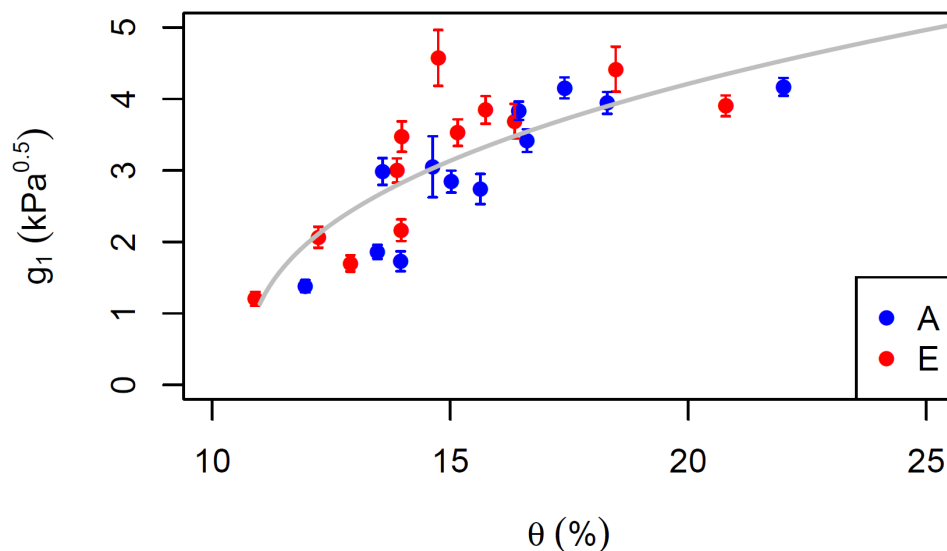
701

702 *Figure 1. Meteorological data measured at the site during the period 2013-2016. Panels show (a) daily mean*  
703 *vapour pressure deficit (D) with shaded area marking the maximum and minimum of the day, (b) daily mean air*  
704 *temperature ( $T_{air}$ ) with shaded area marking the maximum and minimum of the day, (c) daily maximum*  
705 *photosynthetically active radiation (PAR), and (d) monthly total precipitation. Note that precipitation has no*  
706 *direct impact in the model but modifies stomatal conductance via the change in soil moisture.*



707

708 *Figure 2. (a) Leaf area index (LAI) and (b) volumetric water content ( $\theta$ ) used to drive the model. LAI was*  
709 *measured in each ring using the measured absorbed PAR and smoothed using generalized additive model*  
710 *following Duursma et al. (2016).  $\theta$  was measured using neutron probes at top 150 cm biweekly and gap-filled*  
711 *using a linear interpolation between two nearest available data (Gimeno et al. 2018).*



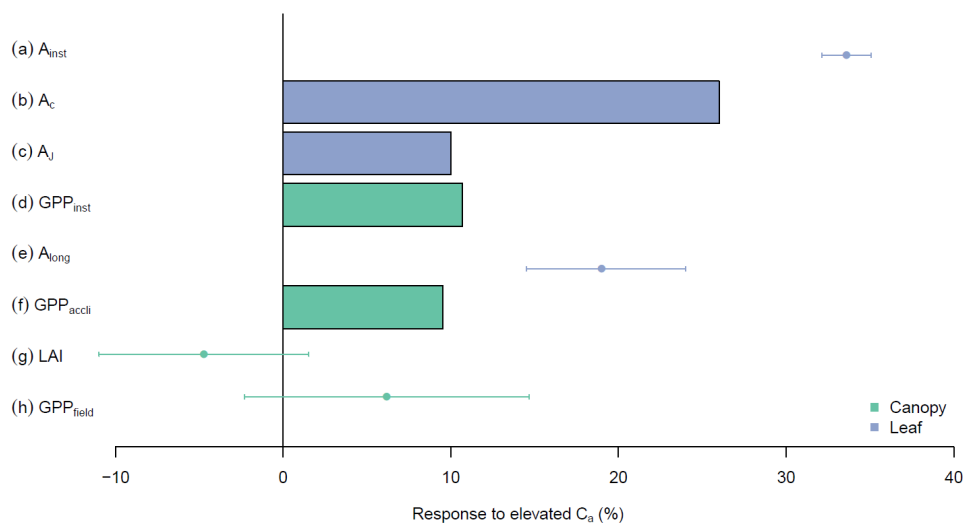
712

713 *Figure 3. The impact of soil moisture content ( $\theta$ ) at top 150 cm on stomatal regulation. Red dots are fitted to*  
714 *data from elevated rings while blue are ambient rings. The bars mark the standard errors of the fitted values.*  
715 *The grey line shows the fit of Eqn. 2 to the data.*



716

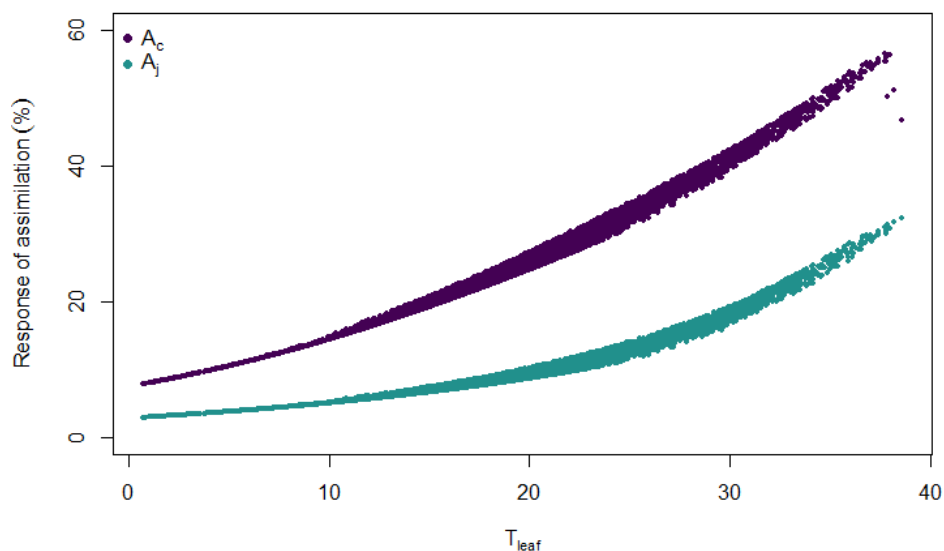
717



718

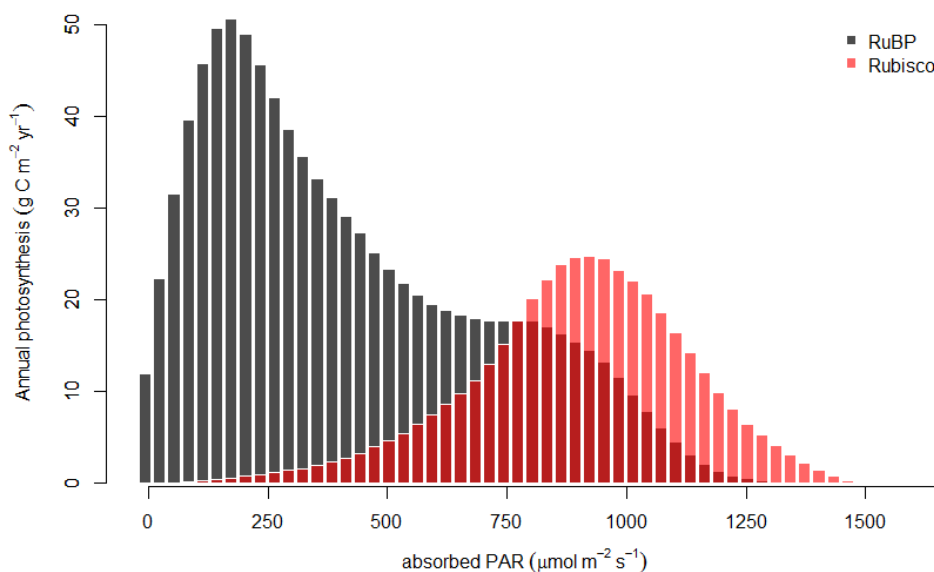
719 *Figure 4. The response of photosynthesis to  $eC_a$  on different scales and limited by different factors. In summary,*  
720 *from top to bottom, the figure demonstrates how a large increase in leaf photosynthesis can diminish into a non-*  
721 *statistically significant change in canopy GPP under  $eC_a$ . Entries from top to bottom are as follows. (a)  $A_{inst}$ , the*  
722 *instantaneous response of leaf photosynthesis to  $eC_a$  obtained from A- $C_i$  measurements in ambient rings (error*  
723 *bars indicate 95% CI). (b)  $A_c$ , the modelled response of Rubisco-limited leaf photosynthesis, assuming no down-*  
724 *regulation, averaged over the range of diurnal air temperatures experienced during the experimental period. (c)*  
725  *$A_j$ , the modelled response of RuBP-regeneration limited leaf photosynthesis. (d)  $GPP_{inst}$ , the direct effect of  $eC_a$*   
726 *on canopy GPP, modelled with MAESPA, assuming no downregulation of photosynthesis and averaged across*  
727 *all six rings. (e)  $A_{long}$ , the long-term response of leaf photosynthesis to  $eC_a$  obtained from leaf photosynthesis*  
728 *measured at treatment  $CO_2$  concentrations (see Ellsworth et al. 2017). This value is different from  $A_{inst}$  because*  
729 *it incorporates photosynthetic acclimation. (f)  $GPP_{long}$ , the effect of  $eC_a$  on canopy GPP once the measured*  
730 *down-regulation of  $V_{cmax}$  is taken into account. (g) LAI, the measured difference in average LAI between  $eC_a$*   
731 *and ambient  $C_a$  rings over the experiment period (data from Duursma et al. 2016). (h)  $GPP_{field}$ , the GPP*  
732 *response modelled with MAESPA comparing the three elevated rings with the three ambient rings. See text for*  
733 *further explanation.*

734



735

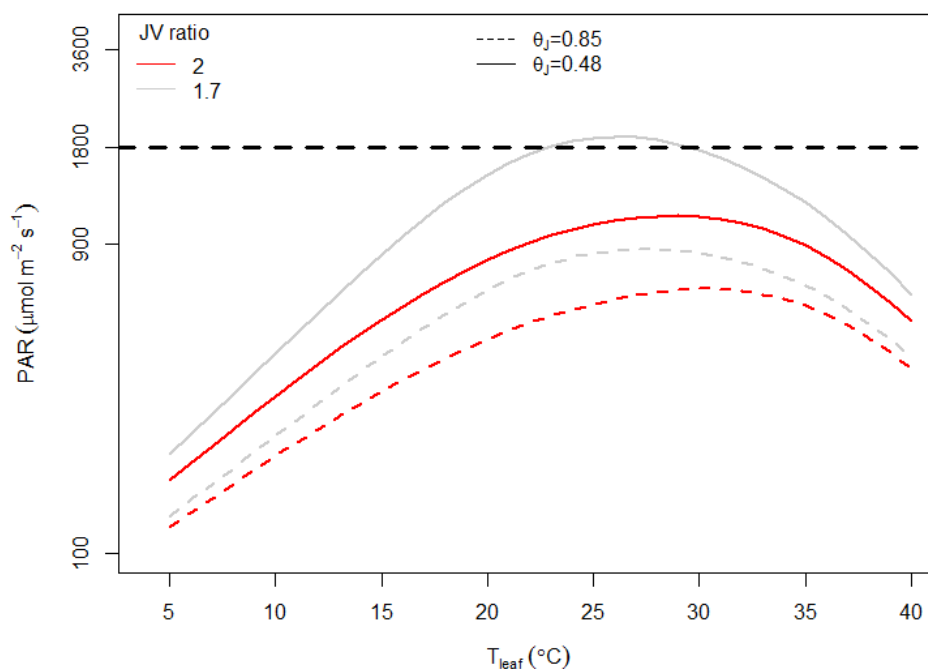
736 *Figure 5. The modelled  $C_a$  response of Rubisco-limited leaf photosynthesis ( $A_c$ ) and RuBP-regeneration-limited*  
737 *leaf photosynthesis ( $A_j$ ) against leaf temperature ( $T_{leaf}$ ). The responses are calculated for temperatures during*  
738 *the period 2013-2016. Parameters are as given in Table 1, except that  $V_{cmax,25}$  and  $g_1$  were assumed to be*  
739 *constant for clarity ( $g_1 = 3.3 \text{ kPa}^{0.5}$  and  $V_{cmax,25} = 90 \mu\text{mol m}^{-2} \text{ s}^{-1}$ ).*



740

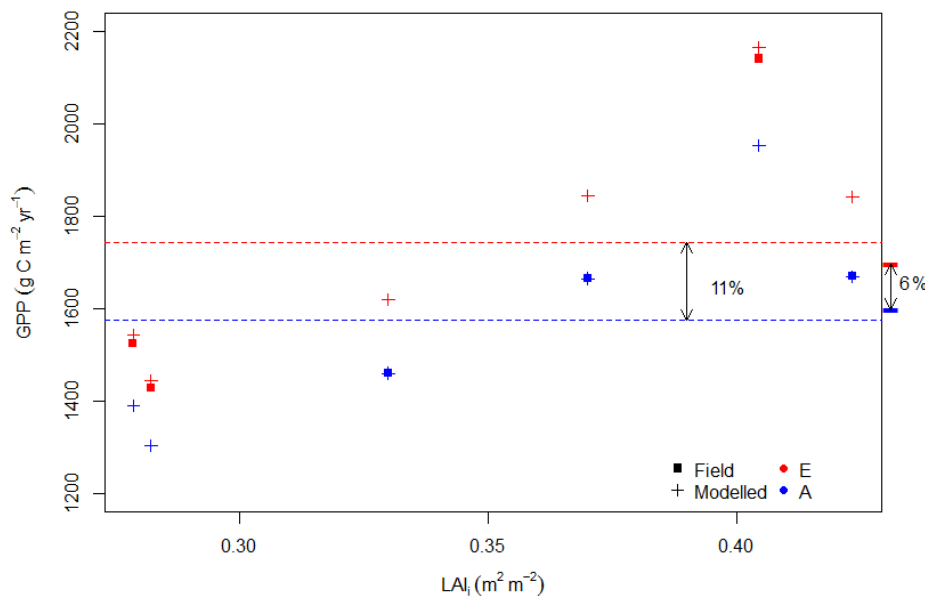


741 Figure 6. Distribution of average annual photosynthesis limited by Rubisco activity and RuBP-regeneration in  
742 bins of absorbed PAR ( $25 \mu\text{mol m}^{-2} \text{s}^{-1}$ ), as calculated by MAESPA across all rings during 2013-2016. The  
743 histogram was constructed by calculating the photosynthesis (either limited by Rubisco or RuBP) falling into  
744 each bin for every half-hour in the “ambient scenario”. These values were then summed to each year and ring  
745 and averaged over six rings and four years.



746

747 Figure 7. Estimated PAR value at which limitation to photosynthesis shifts from RuBP generation to Rubisco at  
748 different leaf temperatures and J:V ratios. Rubisco limitation occurs at PAR values above the curves; RuBP  
749 regeneration limitation occurs below the curves. The curves were calculated using the Photosyn function in the  
750 plantecophys R package (Duursma, 2015). The parameters other than PAR and  $T_{\text{leaf}}$  were assumed to be  
751 constant:  $C_a = 390 \mu\text{mol mol}^{-1}$ ;  $D = 1.5 \text{ kPa}$ ;  $g_1 = 3.3 \text{ kPa}^{0.5}$ ;  $V_{c\text{max},25} = 90 \mu\text{mol m}^{-2} \text{s}^{-1}$ . The temperature and  
752 light dependences of photosynthesis were assumed to be the same as in MAESPA. The grey line was predicted  
753 by assuming  $J_{\text{max},25} = 153 \mu\text{mol m}^{-2} \text{s}^{-1}$  (i.e., J:V ratio = 1.7). This J:V ratio was observed consistently in  
754 EucFACE across campaigns and rings. The red line was predicted by assuming  $J_{\text{max},25} = 180 \mu\text{mol m}^{-2} \text{s}^{-1}$  (i.e.,  
755 J:V ratio = 2). This J:V ratio was commonly reported and used in other studies. The horizontal dashed line  
756 shows the  $\text{PAR} = 1800 \mu\text{mol m}^{-2} \text{s}^{-1}$  at which leaf-level measurements of EucFACE were made. Note the log  
757 scale of the y axis. The dashed curved are based on quantum yield of electron transport ( $\alpha_j$ ;  $\text{mol mol}^{-1}$ ) and  
758 (Convexity of light response of RuBP;  $\theta_j$ ; unitless) values from CABLE model (Haverd et al., 2018).



759  
 760 *Figure 8. The four-year average GPP of all six rings under ambient and eC<sub>a</sub> plotted against initial leaf area*  
 761 *index (LAI<sub>i</sub>). LAI<sub>i</sub> is the LAI measurement taken on the 26 October 2012 and is a proxy of the inherent variation*  
 762 *among the rings. For all six rings, estimated GPP is shown for ambient C<sub>a</sub> (blue) and eC<sub>a</sub> (red). Crosses*  
 763 *indicate GPP from simulations by varying C<sub>a</sub> and squares indicate GPP as under field conditions. The flat bars*  
 764 *on the right hand-side of the plot indicate the average ambient C<sub>a</sub> GPP for ambient rings only (the average of*  
 765 *blue squares) and average eC<sub>a</sub> GPP for elevated rings only (the average of red squares). Dashed lines indicate*  
 766 *average ambient C<sub>a</sub> (the average of blue crosses) and eC<sub>a</sub> GPP across all six rings (the average of red crosses).*  
 767 *The flat bars thus mark the modelled response without inter-ring variability while the dashed lines mark the*  
 768 *modelled realized response, including inter-ring variability.*

769